

Three-dimensional analyses of centrifuge model of embankment on liquefiable soils treated with soil-cement walls

Ross W. Boulanger, Katerina Ziotopoulou
University of California, Davis, CA, USA, rwboulanger@ucdavis.edu

Marie-Pierre Kippen
Gerhart Cole Inc., Salt Lake City, UT, USA

ABSTRACT: Three-dimensional nonlinear dynamic analysis results are presented for a centrifuge model of an embankment on a liquefiable foundation layer treated with soil-cement walls. The analyses were performed using FLAC3D with the user-defined constitutive model PM4Sand3D, which is a newly implemented, generalized version of the plane-strain PM4Sand model. The centrifuge model corresponded to a 28 m-tall embankment underlain by a 9 m-thick saturated loose sand layer. Soil-cement walls were constructed through the loose sand layer near the toe of the embankment and covered with a berm. The model was shaken with earthquake motions having peak horizontal base accelerations of 0.05 g, 0.26 g, and 0.54 g in the first, second, and third events, respectively. The latter two shaking events caused liquefaction in the loose sand layer. The soil-cement walls developed only minor cracks in the second shaking event but were sheared through their full length in the third shaking event. Previous two-dimensional analyses using FLAC with PM4Sand and area-weighted composite properties for the soil-cement treatment zone were able to reasonably approximate the recorded dynamic responses and observed deformation magnitudes but could not capture local deformation mechanisms or directly predict demands on the soil-cement walls. The 3D analyses presented in this paper enabled examination of such details. The favorable agreement between the 3D analysis results and centrifuge model measurements indicates good performance of the PM4Sand3D model and its implementation.

KEYWORDS: liquefaction, earthquake, soil-cement, centrifuge, numerical analysis.

1 INTRODUCTION

Soil-cement grid and wall systems have been used to mitigate the effects of earthquake-induced liquefaction for a wide range of civil infrastructure (Boulanger and Shao 2021). Soil-cement treatments have the advantage that they can be constructed in a range of soil types, including silty soils that can be difficult to treat by densification techniques. The seismic performance of soil-cement grids and walls have been evaluated using three-dimensional (3D) nonlinear dynamic analyses (NDA) (e.g., Bradley et al. 2013, Yamashita et al. 2018), but design practices for embankment dams have generally relied on two-dimensional (2D) approximations with equivalent composite properties for the treatment zones (e.g. Kirby et al. 2010, Friesen and Balakrishnan 2012).

Boulanger et al. (2018) presented centrifuge and numerical simulation results for a 28 m-tall (prototype) embankment on a 9 m-thick liquefiable layer treated with soil-cement walls. The model was shaken with a Kobe motion scaled to peak horizontal base accelerations of 0.05 g, 0.26 g, and 0.54 g in the first, second, and third events, respectively. Two dimensional NDAs using the program FLAC (Itasca) with the user-defined plane-strain PM4Sand model and area-weighted composite properties for the soil-cement treatment zone reasonably approximated the recorded responses and observed deformation magnitudes but could not capture local deformation mechanisms or directly predict demands on the soil-cement walls.

This paper presents results from 3D NDAs of the above-referenced centrifuge model using FLAC3D with the user-defined PMSand3D model. PMSand3D is a newly developed, generalized version of the plane-strain PM4Sand model, for which these analyses represent a first system-level evaluation of its implementation. Representative results are presented for the Kobe 0.26 g and 0.54 g events. The 3D analyses allow examination of more complex local mechanisms, including the extrusion of liquefied sand between the soil-cement walls and the stresses and strains within the soil-cement walls. The favorable agreement between the 3D analysis results and centrifuge model measurements indicates good performance of the PM4Sand3D model and its implementation.

2 PM4SAND3D MODEL

The constitutive model PM4Sand3D is a generalized version of the plane-strain PM4Sand model (Ziotopoulou and Boulanger 2016, Boulanger and Ziotopoulou 2023). These stress-ratio controlled, critical state based bounding surface plasticity models were developed for approximating stress-strain responses important to geotechnical earthquake engineering applications. They require specification of three primary input parameters: apparent relative density, D_r ; shear modulus coefficient, G_0 ; and contraction rate parameter, h_{po} . The optional secondary parameters receive default values if the user does not specify them. The PM4Sand model, with periodic updates since its development in 2010, has been implemented as a user-defined material in a dynamic link library (DLL) for use with the programs FLAC and FLAC2D. Others have implemented PM4Sand in OpenSees and PLAXIS. PM4Sand's plane strain formulation and omission of Lode angle dependency offered computational advantages but limited its use to 2D models. The PM4Sand3D model inherits the features of PM4Sand, adds Lode angle dependency, and is implemented as a user defined material for FLAC3D 9.0 (Itasca 2023). The model's formulation, numerical implementation, and examples of simulated single-element responses for a range of loading conditions are provided in the user manual (Kippen et al. 2026).

3 CENTRIFUGE AND NUMERICAL MODELS

The centrifuge model was tested in a flexible shear beam (FSB) container on the 9 m radius centrifuge at the University of California at Davis. The test results are described in Boulanger et al. (2018) and the data archived in Khosravi et al. (2016).

The configuration of the centrifuge and numerical model is illustrated in Figure 1. Results are presented in prototype dimensions based on standard scaling laws and the centrifugal acceleration of 65 g. The 28 m-tall embankment of dense Monterey sand is underlain by a 9 m-thick saturated loose Ottawa sand layer. Soil-cement walls, 1.4 m-thick and spaced 5.8 m apart (center to center), extend through the loose sand

layer over a 30 m-long interval near the embankment toe. The walls are keyed into a concrete base and covered with a 7.5 m-thick berm. The water has a viscosity of 15 cs and the water table is 1.8 m above the loose sand layer.

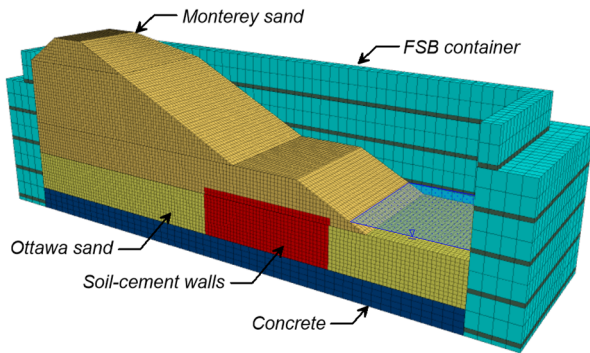


Figure 1. Configuration of centrifuge and FLAC3D model

The model was shaken with a Kobe motion scaled to peak horizontal base accelerations (PBA) of 0.05 g, 0.26 g, and 0.54 g in the first, second, and third events, respectively. The latter two events caused liquefaction in the loose sand layer. Crack detectors in the soil-cement walls showed that they developed only minor cracks in the second shaking event but were sheared through their full length in the third shaking event.

The FSB model container, comprised of hollow rings with rubber spacers, was modeled using solid elastic elements. The solid elastic elements were assigned equivalent solid densities (maintaining total mass) and equivalent flexural moduli (maintaining flexural stiffness along the container length). Container properties are listed in Boulanger et al. (2018).

The Ottawa and Monterey sands were modeled using PM4Sand3D calibrated to the same shear wave velocities (V_s) and cyclic resistance ratios (CRR) as in Boulanger et al. (2018). The Ottawa sand was assigned $D_r = 42\%$ and calibrated to produce $CRR_{15cycles} = 0.093$ at a vertical consolidation stress (σ'_{vc}) of 400 kPa for the first and second event [$G_o = 770$, $h_{po} = 0.21$]. The Ottawa sand was modeled as slightly denser ($D_r = 45\%$) and stronger ($CRR_{15cycles} = 0.12$) for the third event to account for the effects of prior liquefaction [$G_o = 788$, $h_{po} = 0.48$]. The cyclic response of the calibrated model is illustrated in Figure 2. The dense coarse Monterey sand was assigned $D_r = 85\%$ and calibrated to $CRR_{15cycles} = 0.4$ at $\sigma'_{vc} = 400$ kPa for the saturated portion and reasonable drained peak friction angles for the dry portion [$G_o = 1427$, $h_{po} = 2.4$, $n^b = 0.4$].

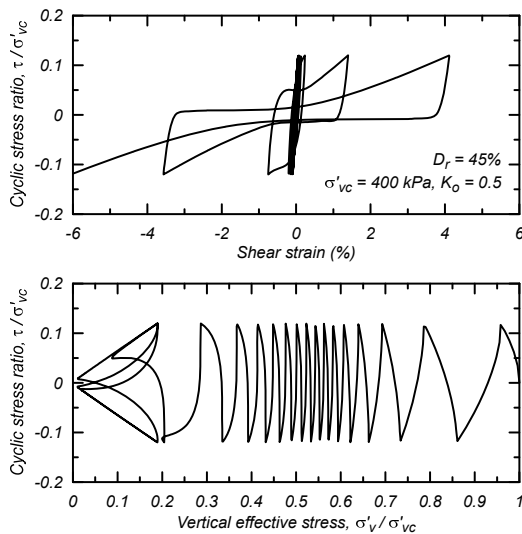


Figure 2. Simulation of undrained cyclic loading response of Ottawa sand in plane-strain simple shear using PM4Sand3D

The soil-cement panels were modeled using an elastic-plastic Mohr-Coulomb model with strain softening. The peak shear strength was set to 1.03 MPa (with friction angle set to zero) based on unconfined compression data. The shear strength was degraded linearly to 60% of its peak value at a cumulative plastic shear strain of 10% (Boulanger and Shao 2021).

Interface elements with a friction angle of 30 degrees and zero cohesion were placed between the soil and FSB container. Interface elements between the soil and soil-cement walls were not included.

4 SIMULATION RESULTS

Numerical simulations were compared to measured responses in terms of the accelerations, pore pressures, displacements, deformation patterns, and soil-cement damage patterns. Representative results are presented herein.

Computed and measured accelerations at three locations on the model for the Kobe 0.26 g and Kobe 0.54 g events are shown in Figure 3 and Figure 4, respectively. The computed accelerations at the top of the berm have stronger higher-frequency components than the measured accelerations, but the accelerations at this and the other locations are otherwise in reasonable agreement with the measured responses.

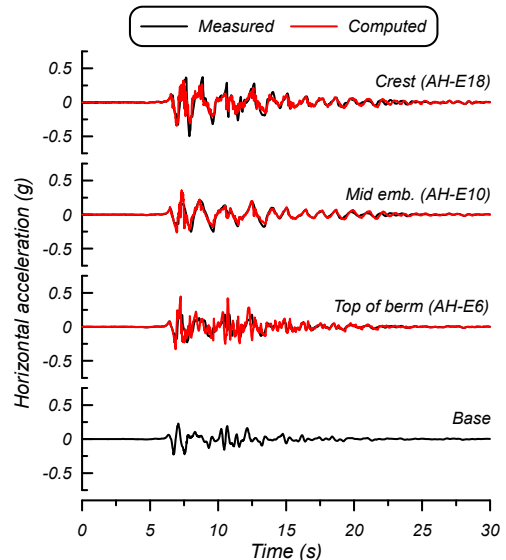


Figure 3. Measured and computed accelerations for Kobe 0.26 g event

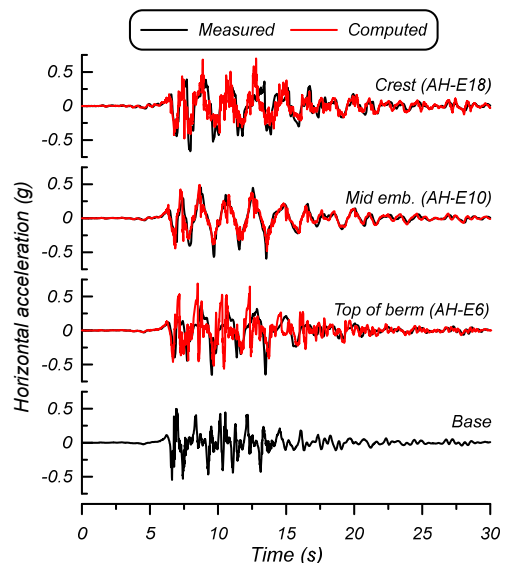


Figure 4. Measured and computed accelerations for Kobe 0.54 g event

Simulated and measured displacements at the embankment crest (settlements) and berm (horizontal displacements) during the Kobe 0.26 g and 0.54 g shaking events are shown in Figure 5 and Figure 6, respectively. The measured displacements are from displacement transducers mounted on racks positioned across the top ring of the container, which moves horizontally relative to the container base during dynamic shaking. Therefore, the computed horizontal displacements are also presented as relative to the top container ring. The crest settlements were underpredicted by about 17% for the Kobe 0.26 g event and overpredicted by about a factor of two for the Kobe 0.54 g event. The horizontal displacement of the berm overlaying the soil-cement section was overpredicted by 8% and 20% for the two events, respectively.

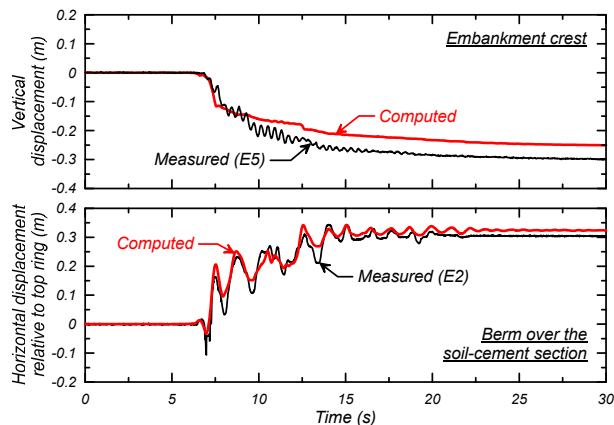


Figure 5. Measured and computed crest settlement and berm horizontal displacement (relative to top ring) for Kobe 0.26 g event

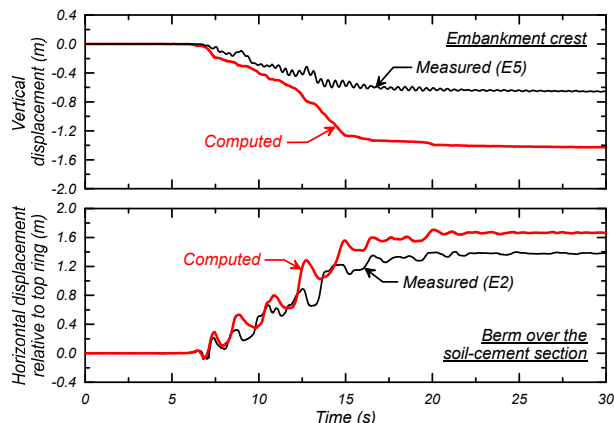


Figure 6. Measured and computed crest settlement and berm horizontal displacement (relative to top ring) for Kobe 0.54 g event

Contours of shear strain at the end of shaking are shown for the Kobe 0.26 g and 0.54 g events in Figure 7. The sections shown in this figure pass through one of the soil-cement walls. The shear strains in the soil-cement walls are greatest just above their connection with the concrete base for both events. These shear strains reach 5-10% in the Kobe 0.26 g event and 35-40% in the Kobe 0.54 g event. Crack sensors embedded in the soil-cement walls indicated minor cracking in the 0.26 g event and full shearing in the 0.54 g event. The post-test excavation photograph in Figure 8 shows the damage to the soil-cement walls from this sequence of shaking events. The simulation results appear reasonably consistent with the observed damage patterns, but do not capture the complexity of the actual cracking and offset patterns. The complexity of the observed damage patterns may be attributable to heterogeneities in the soil-cement and soil properties, neither of which are accounted for in these simulations.

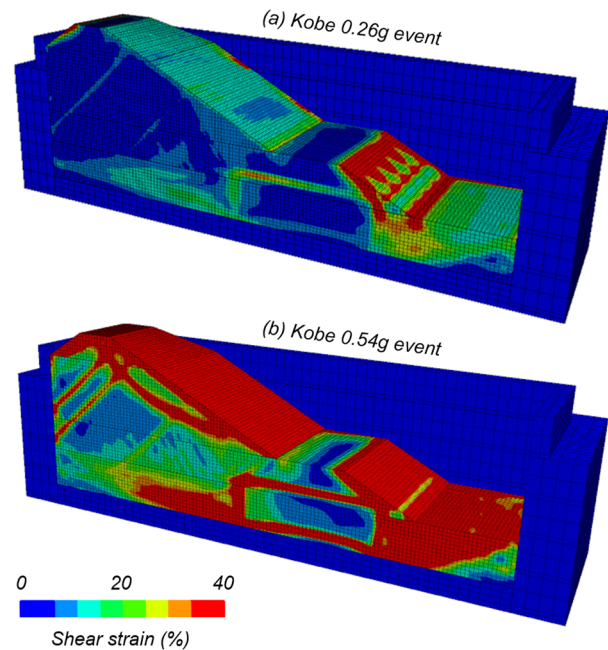


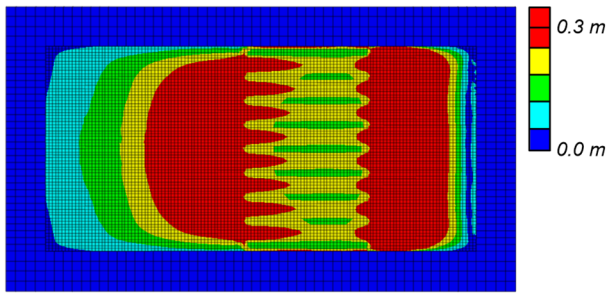
Figure 7. Contours of shear strain at the end of shaking: (a) Kobe 0.26 g event, and (b) Kobe 0.54 g event



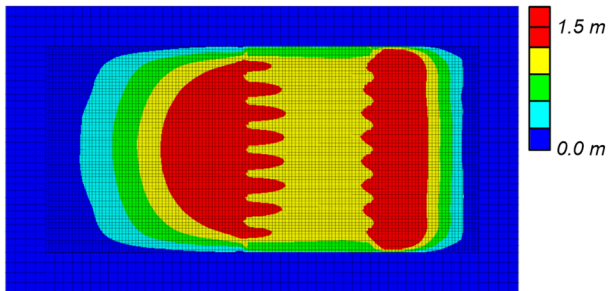
Figure 8. Post-test excavation photo of soil-cement walls from the embankment side looking toward the toe (Boulangier et al. 2018)

Contours of displacement magnitude on a horizontal plane located two-thirds up the soil-cement walls are shown for the Kobe 0.26 g and 0.54 g events in Figure 9. For the Kobe 0.26 g event, the soil-cement walls displaced 0.16-0.18 m, soil between the walls displaced 0.2-0.35 m, and soil immediately upstream and downstream of the walls displaced 0.3-0.5 m. For the Kobe 0.54 g event, the outermost soil-cement walls displaced about 0.8 m, inner soil-cement walls displaced 1.0-1.1 m, soil between the walls displaced 1.0-1.6 m, and the soils immediately upstream and downstream of the walls displaced 1.4-1.8 m. Note that each soil-cement wall is two elements wide and the soil between adjacent walls is six elements wide. The mesh is sufficiently refined to approximate extrusion of sand between the walls, but the omission of interface elements in the present model means that interface slip is not accounted for.

The post-test excavation photo in Figure 10 shows blue paper markers that had been placed flush against the downstream and upstream faces of the soil-cement walls during construction. These markers have been pushed forward between the soil-cement walls by about 0.1 m on the upstream side and pushed away from the walls by up to 0.8 m on the downstream side. The simulation results in Figure 9 are reasonably consistent with the observed pattern of relative displacement between the sand and soil-cement walls and the smaller displacements for the outermost walls (Figure 8).



(a) Kobe 0.26g event



(b) Kobe 0.54g event

Figure 9. Displacement magnitude on a horizontal plane at two-thirds of the soil-cement wall height: (a) Kobe 0.26 g, (b) Kobe 0.54 g

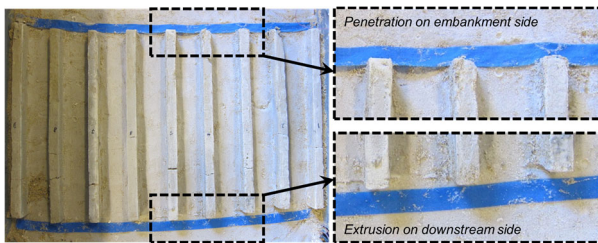


Figure 10. Post-test photo with exposed paper markers (originally aligned in contact with soil-cement wall faces) showing relative movement between the sand and walls (Boulanger et al. 2018)

5 DISCUSSION

Previous 2D analyses of this centrifuge model using FLAC with PM4Sand and area-weighted composite properties for the soil-cement treatment zone were performed by Boulanger and Shao (2021) and Boulanger et al. (2018) with and without strain-softening in the soil-cement, respectively. Those 2D analyses reasonably approximated the recorded dynamic responses and observed deformation magnitudes but could not model local deformation mechanisms or directly predict demands on the soil-cement walls.

The 3D analyses presented herein also reasonably approximated the recorded dynamic responses and observed deformation magnitudes, but it is noteworthy that the degree of agreement is only comparable to, not better than, that obtained with the 2D analyses. Additional sensitivity analyses using the 3D model are in progress. Regardless, the 3D analyses provide improved modeling of the FSB container, soil-container boundary conditions, stresses and strains in the soil-cement walls, and extrusion of the liquefaction sand between soil-cement walls. However, the 3D analyses presented herein do not account for direct slip between the soil-cement walls and liquefied sand, cracking processes in the soil-cement walls (a localization phenomenon that is mesh dependent), diffusion of pore pressures between the soil-cement walls and enclosed liquefying sands, or heterogeneity in the properties of the soil-cement walls or model soils.

6 CONCLUSIONS

Three-dimensional NDA results were presented for a centrifuge model of an embankment on a liquefiable foundation layer treated with soil-cement walls. The analyses were performed using FLAC3D with the user-defined constitutive model PM4Sand3D. The PMSand3D model is a newly developed, generalized version of the plane-strain PM4Sand model, for which these analyses represent a first system-level evaluation of its implementation. The favorable agreement between the 3D analysis results and centrifuge model measurements indicates good performance of the PM4Sand3D model and its implementation.

7 ACKNOWLEDGMENT

The State of California supported the centrifuge tests through the Pacific Earthquake Engineering Research Center (PEER) under project number 1120-NCTRBU. The centrifuge data are archived and publicly available at DesignSafe (PRJ-1277).

8 REFERENCES

- Boulanger, R. W., Khosravi, M., Khosravi, A., and Wilson, D. W. 2018. Remediation of liquefaction effects for an embankment using soil-cement walls: Centrifuge and numerical modeling. *Soil Dynamics and Earthquake Engineering*, 114(2018), 38–50, 10.1016/j.soildyn.2018.07.001.
- Boulanger, R. W., and Shao, L. 2021. Liquefaction mitigation with deep mixing. *Proceedings, Deep Mixing 2021*, Deep Foundations Institute, 1146-1202.
- Boulanger, R. W., and Ziotopoulou, K. 2023. PM4Sand (Version 3.3): *A sand plasticity model for earthquake engineering applications*. Report UCD/CGM-23/01, Center for Geotechnical Modeling, Department of Civil and Environmental Engineering, University of California, Davis, CA.
- Bradley, B. A., Araki, K., Ishii, T., and Saitoh, K. 2013. Effect of lattice-shaped ground improvement geometry on seismic response of liquefiable soil deposits via 3-D seismic effective stress analysis. *Soil Dynamics and Earthquake Engineering*, 48(2013), 35–47.
- Friesen S, and Balakrishnan A. 2012. General approach used for the seismic remediation of Perris Dam. *Proceedings of the 32nd annual USSD conference*, United States Society on Dams.
- Itasca, 2023. *FLAC3D, Fast Lagrangian Analysis of Continua, User's Guide*, Version 9.3. Itasca Consulting Group, Minneapolis, MN.
- Khosravi, A., Khosravi, M., Yunlong, W., Pulido, A., Wilson, D. W., and Boulanger, R. W. 2016. *Remediation of liquefaction effects for a dam using soil-cement walls: Data Report 1: Test AKH01*. Report UCD/CGMDR-16/01, Center for Geotechnical Modeling, University of California, Davis, CA. Curated at DesignSafe-CI [publisher], Dataset, dx.doi.org/10.17603/DS24H50.
- Kippen, M.-P., Boulanger, R. W., and Ziotopoulou, K. 2026. *PM4Sand3D (Version 1): A sand plasticity model for earthquake engineering applications*. Report UCD/CGM-26/01, Center for Geotechnical Modeling, Department of Civil and Environmental Engineering, University of California, Davis, CA.
- Kirby, R. C., Roussel, G. L., Barneich, J. A., Yiadom, A. B., and Todaro, S. M. 2010. Design and construction of seismic upgrades at San Pablo Dam using CDSM. *Proceedings of the 30th Annual USSD Conference*, United States Society on Dams, 137–151.
- Yamashita, K., Shigeno, Y., Hamada, J., and Chang, D.-W. 2018. Seismic response analysis of piled raft with grid-form deep mixing walls under strong earthquakes with performance-based design concerns. *Soils and Foundations*, Elsevier, 58(2018), 65–84.
- Ziotopoulou K. and Boulanger, R. W. 2016. Plasticity modeling of liquefaction effects under sloping ground and irregular cyclic loading conditions. *Soil Dynamics and Earthquake Engineering*; 84:269-283, 10.1016/j.soildyn.2016.02.013.